Original Investigation

DOI: 10.4274/jarem.galenos.2024.66199

J Acad Res Med

# Utility of Relative ADC in Discriminating the Benign and Malign Liver Masses: Diagnostic Potential in Comparison to ADC

Neşe Uçar[1], Levent Karakaş[1], Ebru Yılmaz[2], Elif Evrim Ekin[3], Aylin Hasanefendioğlu Bayrak[4], Hüseyin Özkurt[5]

[1]University of Health Sciences Turkey, Gaziosmanpaşa Training and Research Hospital, Clinic of Radiology, İstanbul, Turkey
[2]Acıbadem University Altunizade Hospital, Clinic of Radiology, İstanbul, Turkey
[3]Hisar Intercontinental Hospital, Clinic of Radiology, İstanbul, Turkey
[4]University of Yeni Yüzyıl Gaziosmanpaşa Hospital, Department of Radiology, İstanbul, Turkey
[5]University of Health Sciences Turkey, İstanbul Seyrantepe Hamidiye Etfal Training and Research Hospital, Clinic of Radiology, İstanbul, Turkey

**Cite this article as:** Uçar N, Karakaş L, Yılmaz E, Ekin EE, Hasanefendioğlu Bayrak A, Özkurt H. Utility of Relative ADC in Discriminating the Benign and Malign Liver Masses: Diagnostic Potential in Comparison to ADC.

## ABSTRACT

**Objective:** The aim of this study was to compare the utility of apparent diffusion coefficient (ADC) and relative ADC (rADC) values in differentiating benign and malignant liver masses and retrospectively evaluate the diagnostic contribution of rADC values.

**Methods:** We evaluated 92 focal liver lesions in 56 patients (27 females and 29 males) who were histopathologically diagnosed or did not increase in size on follow-up imaging. Diffusion-weighted images were acquired at two different b values (b=0 and b=800 s/mm$^2$) and mean ADC values and rADC values obtained from ADC maps with renal cortex as the reference organ were measured. Receiver operating characteristic curve analysis was performed to determine the ADC and rADC cut-off values. Diagnostic values and confidence intervals were obtained. P<0.05 was accepted as the level of statistical significance.

**Results:** The mean ADC values of benign and malignant lesions were 1.66±0.49x10$^{-3}$ mm$^2$/s and 1.04±0.24x10$^{-3}$ mm$^2$/s, respectively. The sensitivity and specificity of ADC at a cut-off value of 1.149x10$^{-3}$ mm$^2$/s were 88% and 77%, respectively. The mean rADC was 0.88±0.25 for benign lesions and 0.57±0.15 for malignant lesions. The sensitivity and specificity of the rADC at a cut-off value of 0.62 were 95% and 72%, respectively.

**Conclusion:** rADC was not significantly superior to ADC in the differentiation of benign and malignant lesions. Both ADC and rADC values show high sensitivity and specificity for the differentiation of benign and malignant liver lesions. They are recommended to be used together in cases of suspected malignancy.

**Keywords:** Apparent diffusion coefficient, hemangioma, hepatic metastasis, hepatocellular carcinoma, magnetic resonance imaging

## INTRODUCTION

Accurate detection of malignant liver lesions such as hepatocellular carcinoma (HCC) and metastases is of critical importance in optimal patient management (1,2).

Magnetic resonance imaging (MRI) is often used to characterize liver masses detected by ultrasonography or computed tomography. In the characterization of liver lesions, mass morphology; signal intensity, and enhancement patterns are evaluated on conventional MRI sequences. Diffusion-weighted imaging (DWI) has recently been added to the abdominal MRI protocol (3). DWI is an advanced imaging method that provides important information about the diagnosis of the mass, prognosis, treatment planning, and response to treatment. Its benefits have also been demonstrated in patients with contraindications to gadolinium contrast agents (4). The diffusion imaging technique is based on the evaluation of random movements of water molecules in the environment driven by kinetic energy and is quantitatively evaluated by measuring the ADC value. In most malignant lesions, diffusion is restricted due to increased

**ORCID IDs of the authors:** N.U. 0000-0003-2233-4338; L.K. 0000-0001-5485-9337; E.Y. 0000-0001-8681-1565; E.E.E. 0000-0003-1290-6291; A.H.B. 0000-0003-4644-6318; H.Ö. 0000-0001-6600-4571.

**Corresponding Author:** Neşe Uçar,
E-mail: neseyigit@hotmail.com

**Received Date:** 07.03.2024 **Accepted Date:** 09.04.2024

cellularity and disruption of the extracellular space, resulting in low ADC values (5). Different ADC values have been reported for different cancer tissues in previous studies (6,7). These differences in ADC values may be due to patient-related factors, such as age and body temperature, or technical differences, such as variations in the region of interest (ROI) area measurement and the use of different b values during the formation of ADC maps (8-12). The use of relative ADC is recommended to minimize variability and optimize the ADC value. The relative ADC is calculated using the formula $ADC_{mass}/ADC_{reference\ organ}$.

In previous studies, adjacent parenchymal tissue, contralateral tissue, or different organs have been used as reference organs for rADC, and the contribution of rADC to the diagnosis has been reported (13-17). The spleen and renal cortex have been used as reference organs in liver MRI (18-20). As it is associated with the most distinctive anatomical borders in the ADC map and the lowest coefficient of variation, the renal cortex has been considered to be the most suitable reference organ in the abdomen for the calculation of relative ADC (21).

We aimed to evaluate the diagnostic utility of rADC in discriminating the benign and malignant liver masses on DWI by comparing the ADC values with the rADC values obtained by considering the renal cortex as the reference organ.

## METHODS

This retrospective single-center study was approved by the University of Health Sciences Turkey, Taksim Training and Research Hospital Ethics Committee (decision no: 7, date: 13. 05.2015). Informed consent forms were obtained from all.During a 24-month period (January 2013 to February 2015), 80 patients were referred to our center for liver MRIs. Patients with severe motion artifacts (n=9) and renal parenchymal disease (n=3) or those who had received chemotherapy within the last 12 months (n=12) were excluded from the study. The inclusion criteria were as follows: lesions larger than 1 cm; histopathologically proven malignant liver masses; benign masses with typical MRI signal characteristics, no size change on follow-up imaging, or histopathologically proven. Histopathological was examined for 43 lesions (46.7%), while the remaining were followed up throughout the 3-year period at 12-month intervals. Consequently, 92 lesions in 56 patients (27 women and 29 men) were included in the study.

Benign lesions involved simple liver cyst (n=5), hemangioma (n=25), focal nodular hyperplasia (FNH) (n=8), hydatid cyst (n=2), adenoma (n=3) and angiomyolipoma (n=1) while malignant lesions were metastases (colorectal cancer n=19, gastric cancer n=2, pancreatic cancer n=4, breast cancer n=5), HCC (n=14), FHCC (n=1) and cholangiocarcinoma (n=3).

Simple liver cysts and hemangiomas were diagnosed based on typical MRI findings (3). Two cases of hydatid cysts were diagnosed with typical radiological features [cystic echinococcosis (CE3a)] (22). The diagnoses of FNHs were confirmed by biopsy and imaging features on T1-T2W images and contrast enhancement patterns on dynamic MRI (16). One patient with FNH had undergone surgical resection because of the increased lesion size during the follow-up period. Other FNHs remained stable in size at follow-up. The diagnosis of other benign solid liver masses was confirmed either by biopsy or surgery. Adenomas showed heterogeneous signal intensity on T1-T2W images and intense contrast enhancement in dynamic post-contrast sequences. Hepatic angiomyolipoma was observed as signal drop out on out-of-phase imaging due to the presence of fat.

Malignant masses were histopathologically confirmed. In metastatic lesions, the pathological diagnosis of the largest lesion was confirmed. HCCs were enhanced early after intravenous contrast administration and became hypointense on delayed images, except for five lesions. These lesions exhibited an atypical enhancement pattern. Alpha-fetoprotein levels were high in patients diagnosed with HCC. All patients who had HCC, except one, had chronic liver disease. Four patients had single masses and the others had multifocal masses. Follow-ups of patients with known primary malignancies detected 30 metastases that showed pathologic tracer uptake on positron emission tomography/computed tomography. Fibrolamellar hepatocellular carcinoma (FHCC) was a large mass with a central scar and calcifications. Cholangiocarcinomas showed peripheral and delayed contrast enhancement. These masses were located peripherally, and two of them showed capsular retraction.

### MRI Protocol

All was examined using 1.5-T systems (Magnetom Avanto, Siemens Healthcare, Germany). DWI was performed using a single-shot echo-planar imaging fat-suppressed sequence in the axial plane during a single end-expiratory breath-hold using the following parameters: TR/TE, 6000-72; slice thickness, 7 mm; interslice gap, 1.4 mm; field of view, 485x379 mm; matrix, 192x120 and bidirectional gradients in x, y, and z directions were acquired using the following b values: 0, 800 s/mm$^2$. ADC maps were prepared using these images. The routine MR sequences also included coronal T2W turbo spin-echo with fat suppression half-Fourier acquisition single-shot turbo spin-echo, axial fat-suppressed T2W turbo spin-echo with the BLADE technique, gradient-recalled echo T1W in-phase and out-of-phase, and unenhanced and contrast-enhanced 3D T1W gradient-echo [volumetric interpolated breath-hold examination VIBE)]. After contrast agent administration, VIBE T1W sequences were acquired in different phases. As a nonspecific agent, Gd-BT-DO3A (Gadovist, Bayer Schering Pharma, Germany) and as a liver-specific agent, EOB-Gd-BPTA (Primovist, Bayer Schering Pharma, Germany) were employed. The liver-specific agent was used in 38 patients.

### Apparent Diffusion Coefficient Analysis

The DWI data were transferred to a workstation (syngo. via; Siemens Healthcare, Erlangen, Germany), and the average ADC values of all lesions were measured using these maps. The ADC is calculated according to the equation ADC =-1/(b2-b1)ln(S2/S1); S1 and S2 are the signal intensities in the regions of interest with

two different b values (b1=0 s/mm$^2$ and b2=800 s/mm$^2$). Circular ROIs of at least 20 mm$^2$ were inserted by one radiologist (N.U.) to measure ADC and rADC values. Normal liver parenchymal tissue and necrotic areas were not included in the T2W and post-gadolinium T1W images in ADC measurements. Three measurements were performed, and the lowest mean ADC value was set. In the calculation of the relative ADC, the ADC value obtained from the right renal cortex was used. The ratio of the ADC value of the liver lesion to the ADC value of the renal cortex was considered as the rADC value.

### Statistical Analysis

Data were analyzed using IBM SPSS Statistics Standard Concurrent User V 26 (IBM Corp., Armonk, New York, USA) and MedCalc® Statistical Software version 19.6 (MedCalc Software Ltd, Ostend, Belgium) statistical package programs. Descriptive statistics are given as the number of units (n), percentage (%), mean (X), standard deviation, median, minimum, and maximum values.

In addition, Kolmogorov-Smirnov normality test results showed that the data conformed to a normal distribution (p=0.053 for ADC, p=0.200 for rADC). In the comparison of lesion groups, independent sample t-test was used for normally distributed variables and Mann-Whitney U test was used for non-normally distributed variables. Pearson's chi-square test was used to compare lesion groups by gender. The performance of ADC and rADC in predicting lesion groups was evaluated by receiver operating characteristic curve analysis. The optimum cut-off value was determined as the value with the maximization of the sum of the sensitivity and specificity values. P<0.05 was considered statistically significant.

## RESULTS

A total of 56 patients, 28 in the benign group and 28 in the malignant group, were included in the study. The median age of the patients in the benign group was 45 years and 50 years in the malignant group. The number of male patients was 14 (50%) in the benign group and 15 (53.6%) in the malignant group. The number of female patients was 14 (50%) in the benign group and 13 (46.4%) in the malignant group. The descriptive characteristics of the patients in the lesion groups had a similar (homogeneous) distribution (p>0.05) (Table 1). A total of 92 lesions were evaluated in patients, 44 in the benign group and 48 in the malignant group. The median number of lesions in the benign and malignant groups was 1. In the benign group, 25 (56.8%) hemangiomas, 8 (18.2%) FNHs, 7 (15.9%) cystic lesions, and 4 (9.1%) other solid benign lesions were observed. In the malignant group, there were 15 (31.3%) HCC, 3 (6.3%) cholangiocarcinomas, and 30 (62.5%) metastatic lesions. While the number of lesions in the groups had a similar (homogeneous) distribution (p>0.05), the types of lesions were different in the two groups (p<0.05) (Table 2).

The mean ADC was 1.66±0.49x10$^{-3}$ mm$^2$/s for benign lesions and 1.04±0.24 02x10$^{-3}$ mm$^2$/s for malignant lesions. Mean ADC was statistically higher in the benign group than in the malignant group (p<0.001). The mean rADC was 0.88±0.25 and 0.57±0.15 for the benign and malignant groups, respectively. The mean ADC was statistically higher in the benign group than in the malignant group (p<0.001). The mean ADC of all lesions was 1.34±0.49x10$^{-3}$ mm$^2$/s and the mean rADC was 0.72±0.25 (Table 3).

The area under the curve (AUC) value for ADC was 0.898 (p<0.001). The optimum cut-off value for the ADC value was obtained as 1.149x10$^{-3}$ mm$^2$/s. According to this value, the sensitivity was 88.65% and the specificity was 77.08%. The AUC value for rADC was 0.890 (p<0.001). Sensitivity was 95.45% and specificity was 72.92%, using an optimum cut-off value of 0.62 for rADC. When the confidence intervals for AUC are analyzed, the AUC confidence intervals for ADC and rADC intersect. Accordingly, while ADC and rADC values showed similar effects in differentiating benign and malignant groups, they were not significantly superior to each other (Table 4) (Figure 1).

Cystic lesions showed the highest mean ADC and rADC values in the benign lesions group. The mean ADC and rADC values of liver hemangiomas were higher than those of other benign solid lesions (Figure 2,3). Mean ADC and rADC values of FNHs and other solid benign lesions were higher than those of malignant lesions (Figure 4). The mean ADC and rADC values of HCCs were higher than those of other malignant lesions (Figure 5). There were overlaps between the ADC values of solid benign and solid malignant subtype lesions.

**Table 1. Comparison of demographic characteristics of patients according to lesion groups**

| | Group | | All patients | Test (p) |
|---|---|---|---|---|
| | Benign | Malign | | |
| | n=28 | n=28 | n=56 | |
| **Age, (year)** | | | | z=-1.617 p=0.106 |
| **M (IQR)** | 45 (13) | 50 (11) | 49 (13) | |
| **Gender, n (%)** | | | | $\chi^2$=0.072 p=0.789 |
| Male | 14 (50%) | 15 (53.6%) | 29 (51.8%) | |
| Female | 14 (50%) | 13 (46.4%) | 27 (48.2%) | |

Mann-Whitney U test (z); chi-square test (Pearson chi-square) ($\chi^2$); M: median, IQR: interquartile range, n: number of patients, %: percentage

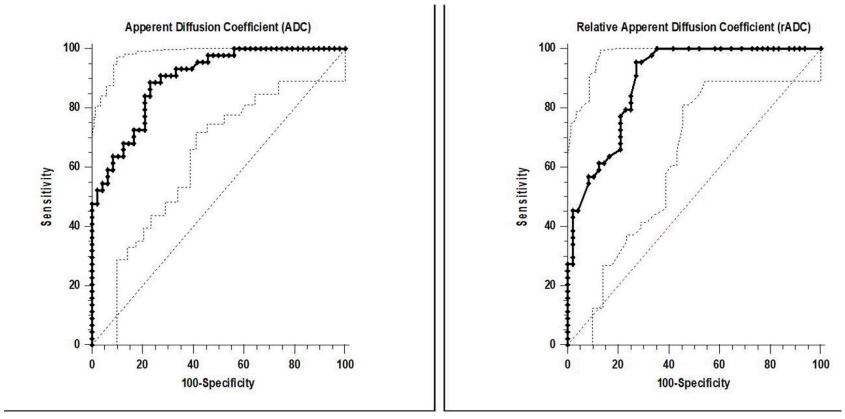


**Figure 1.** ROC curve for ADC and rADC
*ROC: receiver operating characteristic*

**Table 2. Comparison of types of lesions of patients according to lesion groups**

| | Group | | All lesions | Test (p) |
|---|---|---|---|---|
| | Benign | Malign | | |
| Number of lesions, n | 48 | 44 | 92 | z=-0.834 p=0.404 |
| M (IQR) | 1 (1) | 1 (2) | 1 (1) | |
| **Type of lesions, n (%)** | | | | - |
| Hemangioma | 25 (56.8%) | 0 (0%) | 25 (27.2%) | |
| FNH | 8 (18.2%) | 0 (0%) | 8 (8.7%) | |
| Cystic lesions* | 7 (15.9%) | 0 (0%) | 7 (7.6%) | |
| Other solid benign lesions** | 4 (9.1%) | 0 (0%) | 4 (4.3%) | |
| HCC | 0 (0%) | 15 (31.3%) | 15 (16.3%) | |
| Cholangiocarcinoma | 0 (0%) | 3 (6.3%) | 3 (3.3%) | |
| Metastasis | 0 (0%) | 30 (62.5%) | 30 (32.6%) | |

Mann-Whitney U test (z); M: median, IQR: interquartile range, n: number of patients, %: percentage
*Cystic lesions refer simple cyst and hydatid cyst. **Other solid benign lesions refer adenoma and angiomyolipoma

**Table 3. Comparison of mean ADC and rADC values between benign and malignant groups**

| | Group | | All of lesions | Test (p) |
|---|---|---|---|---|
| | Benign | Malign | | |
| | n=44 | n=48 | n=92 | |
| **ADC ($10^{-3}$ mm²/s)** | | | | **t=7.710 p<0.001** |
| X ± SD | 1.66±0.49 | 1.04±0.24 | 1.34±0.49 | |
| **rADC** | | | | **t=7.294 p<0.001** |
| X ± SD | 0.88±0.25 | 0.57±0.15 | 0.72±0.25 | |

Independent sample t-test (t); descriptive statistics are given as mean (X) and standard deviation (SD) values. ADC: apparent diffusion coefficient, rADC: relative ADC

**Table 4. ROC curve analysis findings for ADC and rADC values**

| | Cut-off | Sensitivity (95% CI) | Specificity (95% CI) | AUC (95% CI) | p-value |
|---|---|---|---|---|---|
| ADC ($10^{-3}$ mm²/s) | >1.149 | 88.64 (75.4-96.2) | 77.08 (62.7-88.0) | 0.898 (0.817-0.951) | **<0.001** |
| rADC | >0.62 | 95.45 (84.5-99.4) | 7.92 (58.2-84.7) | 0.890 (0.808-0.946) | **<0.001** |

ROC: receiver operating characteristic, ADC: apparent diffusion coefficient, rADC: relative ADC, AUC: area under the curve, CI: confidence interval

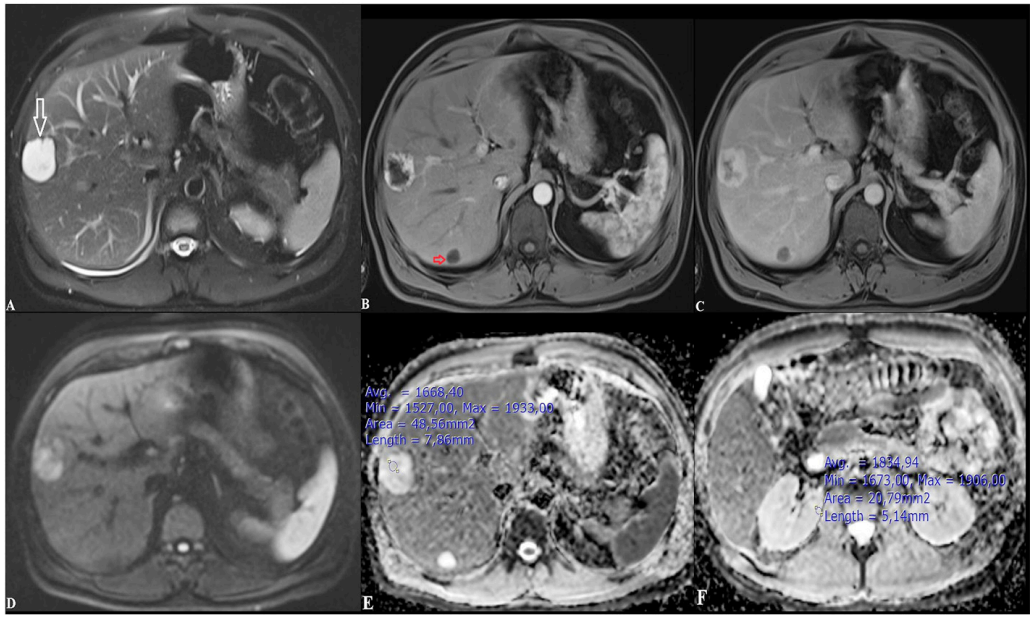


**Figure 2.** 53-year-old male patient with rapidly enhancing hemangioma. A. T2W fat-saturated image demonstrates a well-defined hyperintense lesion (white arrow). B. In arterial phase of dynamic MRI, a typical peripheral nodular contrast-enhancement pattern is observed. Also, a simple cyst can be seen (small arrow). C. In portal phase, rapidly contrast enhancement is seen. D. DWI (b-value of 800 s/mm2) shows hyperintensity. E-F. On the corresponding ADC map, the hemangioma shows high ADC and rADC values

*ADC: apparent diffusion coefficient, rADC: relative ADC, MRI: magnetic resonance imaging, DWI: diffusion-weighted imaging*

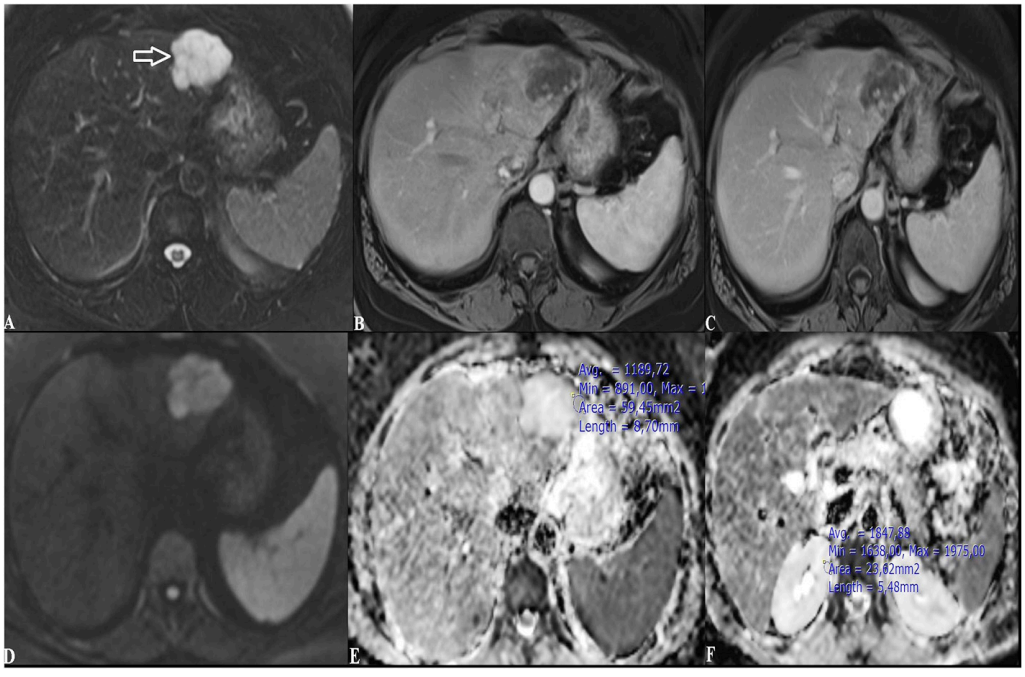


**Figure 3.** 52-year-old female patient with slowly enhancing hemangioma. A. T2W fat-saturated image shows hyperintense lesion (white arrow). B-C. On dynamic contrast-enhanced MRI images are observed peripheral nodular discontinuous enhancement which slowly progresses centripetally. D. DWI (b-value of 800 s/mm$^2$) shows heterogeneous hyperintensity. E-F. The ADC value of the lesion was below the cut-off value, and rADC was above the cut-off value

*ADC: apparent diffusion coefficient, rADC: relative ADC, MRI: magnetic resonance imaging, DWI: diffusion-weighted imaging*

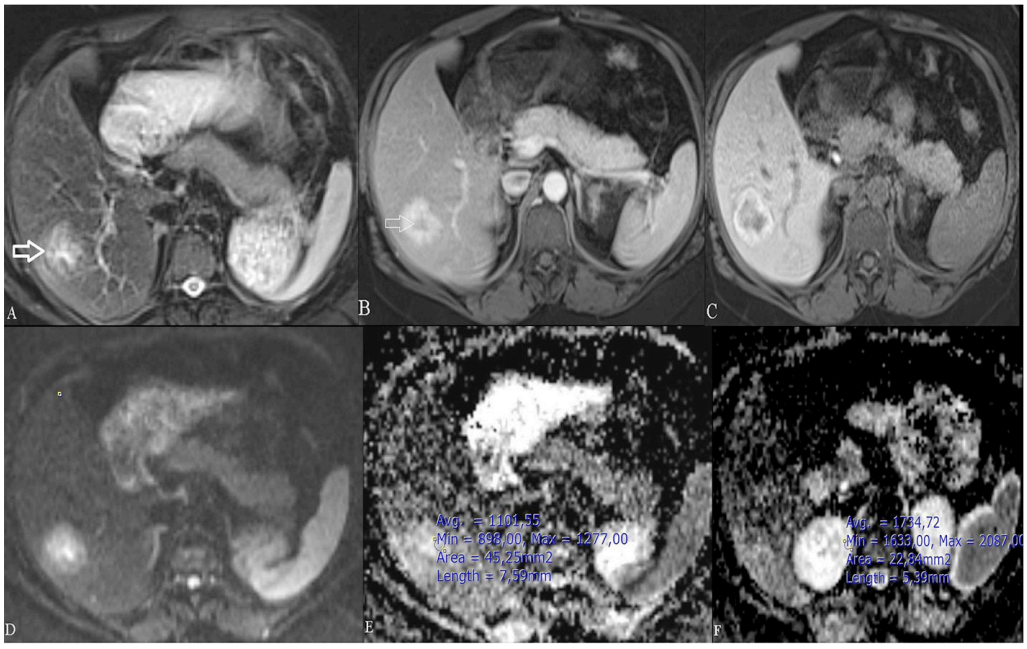


**Figure 4.** 29-year-old female patient with FNH. A. T2W fat-saturated image shows heterogeneous hyperintense lesion (white arrow). B. In a portal phase of dynamic MRI, Intense enhancement and central fibrotic scar are seen (thin white arrow). C. Hepatobiliary phase on contrast-enhanced MRI demonstrates hyperintensity on the outer layer. D. DWI (b-value of 800 s/mm$^2$) shows hyperintensity. E-F. The FNH shows low ADC and rADC values

*FNH: focal nodular hyperplasia, ADC: apparent diffusion coefficient, rADC: relative ADC, MRI: magnetic resonance imaging, DWI: diffusion-weighted imaging*

## DISCUSSION

DWI is an advanced imaging method that aids in the differential diagnosis of focal liver lesions when used together with routine sequences in MRI. ADC values of benign and malignant focal liver lesions have been compared in prior publications (23-25). Several studies have shown that the ADCs of benign hepatic lesions may overlap with those of malignant lesions (26,27).

As mentioned above, technical differences and patient-related factors may cause variability in ADC values. The primary purpose of using the relative ADC value is to establish a threshold value independent of technical limitations and patient factors. It was stated that the renal medulla of the kidney showed anisotropic diffusion because of the radial orientation of its structures (10). Therefore, the ADC value obtained from the right renal cortex, avoiding the renal medulla as the reference organ, was used to calculate the relative ADC. Our findings regarding the potential utility of the rADC value in the diagnosis of liver lesions revealed that both ADC ($p<0.001$) and rADC ($p<0.001$) values can be used in the discriminating the benign and malignant liver lesions, with no significant superiority of rADC over ADC.

The contribution of the rADC value to diagnosis has been investigated in various studies. Do et al. (18) calculated the rADC values using the spleen as a reference organ in the evaluation of liver fibrosis and demonstrated that the rADC value increased the diagnostic accuracy in the detection of liver fibrosis. Park et al. (21) determined the renal cortex as the reference organ with the highest reproducibility in the first series of their studies, and then in the second series by comparing the ADC and rADC values of metastatic and non-metastatic lymph nodes in 130 patients with uterine cervical cancer, they reported the likelihood of the rADC value to increase the accuracy of the diagnosis of metastatic lymph nodes.

Hong et al. (20) compared liver ADC and rADC values to evaluate liver fibrosis via 3 Tesla MRI in chronic hepatitis B patients. Liver ADC and rADC values (specifically, S-rADC and R-rADC values, defined as the ratio of the liver ADC to the spleen and renal cortex ADC values, respectively) were measured and compared with METAVIR liver fibrosis scores. The results showed that R-rADC at b=600 s/mm$^2$ was more accurate in predicting the stages of hepatic fibrosis. The renal cortex has been suggested as a reference organ (20).

In this study, all simple cysts, two hydatid cysts, and one angiomyolipoma showed higher ADC and rADC values consistent with benignity. In addition, while FNHs showed the lowest ADC and rADC values in the benign group, they overlapped with malignant lesions. Previous studies have reported that the ADC values of some benign lesions, such as FNH and adenoma, overlap with the ADCs of malignant lesions (26,27). These findings were attributed to the hypercellularity of FNHs, which resulted in restricted diffusion. However, in our study, the ADC and rADC values of adenomas were in the benign group. The reason for this could be explained by the lower number of cysts in our study and the relatively higher

mean ADC values of adenomas because of the decrease in our cut-off value due to solid lesions.

Wu et al. stated that the difficulty in distinguishing atypical hemangiomas from colorectal cancer metastases might lead to misdiagnosis and unnecessary surgical resection (28). Nam et al. (29) divided 69 hemangiomas into three groups to evaluate the ratio of total tumor volume to the visually estimated contrast increase in portal phase images, and contrast enhancement of >75% was classified as group 1, those with 25-75% as group 2, and those with 25% as group 3. The lowest ADC values were calculated in group 3, and a significant difference was observed between groups 1 and 3. They reported that restricted diffusion may be due to structural differences in hemangiomas (29). In this study, we observed that the ADC values were below the cut-off value in four of the 25 hemangiomas. These lesions were above the cut-off value determined for the rADC values. The enhancement features of these lesions with low ADC values and suspected malignancy were compatible with group 3. This result suggested that the rADC value may be superior to the ADC value in terms of contribution to diagnosis. We then evaluated the contribution of rADC to the differentiation of hemangiomas and malignant masses. However, no statistical difference was observed.

Evaluation of the malignant lesions included in our study revealed that the ADC and rADC values of five colorectal cancer metastases were above the cut-off value. In a study by Cui et al. (30), 87 colorectal and gastric hepatic metastases were divided into two groups as lesions responsive to and non-responsive to chemotherapy according to ADC values before and during treatment. The authors reported that nonresponsive lesions had higher pretreatment mean ADC values than responding lesions and stated that high ADC values may be associated with necrotic areas (30). In our study, in contrast to the study by Cui et al. (30), measurements were performed from ROI areas that did not cover the entire tumor but included the peripheral parts with the most restricted diffusion and with exclusion of the cystic or necrotic components. It has been reported that metastatic liver lesions may be perfused by vessels originating from the lower oxygenated portal venous system, leading to the formation of hypoxic tissue in the tumor (31). In addition, the presence of viable hypoxic cells around the necrotic areas developing in the tumor causes the development of hypoxia-related treatment resistance (32). A moderate correlation between ADC values and tumor hypoxia levels was reported in an animal model study (33). Accordingly, in the current study, the identification of high ADC values in all five lesions and concomitantly high rADC values in all lesions may be related to the ADC variability of the hypoxic areas resulting from decreased perfusion of the tumor.

### Study Limitations

There are several limitations to this study, such as the small sample size, particularly in the benign group, and the inability to include lesions 1 cm because of limited spatial resolution in diffusion sequences. In addition, the images were analyzed by one radiologist in our study; therefore, the intra- and interobserver variability of ADC measurements could not be tested. It would be better to include a larger-scale study population in future studies.

## CONCLUSION

Both ADC and rADC values can be used to differentiate benign and malignant lesions with high sensitivity and specificity. The combined use of ADC and rADC values for lesions with suspected malignancy is recommended because of their advantages in different cases.

**Ethics Committee Approval:** Study was approved by the University of Health Sciences Turkey, Taksim Training and Research Hospital Ethics Committee (decision no: 7, date: 13. 05.2015).

**Informed Consent:** Informed consent forms were obtained from all.

**Author Contributions:** Surgical and Medical Practices - N.U., E.Y., E.E.E.; Concept - H.Ö.; Design - N.U., H.Ö.; Data Collection and/or Processing - N.U., L.K.; Analysis and/or Interpretation - L.K., A.H.B.; Literature Search - N.U., A.H.B.; Writing - N.U., E.E.E.

**Conflict of Interest:** The authors have no conflict of interest to declare.

**Financial Disclosure:** The authors declared that this study has received no financial support.

## REFERENCES

1. Crissien AM, Frenette C. Current management of hepatocellular carcinoma. Gastroenterol Hepatol (N Y) 2014; 10: 153-61.
2. Sica GT, Ji H, Ros PR. CT and MR imaging of hepatic metastases. AJR Am J Roentgenol 2000; 174: 691-8.
3. Matos AP, Velloni F, Ramalho M, AlObaidy M, Rajapaksha A, Semelka RC. Focal liver lesions: Practical magnetic resonance imaging approach. World J Hepatol 2015; 7: 1987-2008.
4. Galea N, Cantisani V, Taouli B. Liver lesion detection and characterization: role of diffusion-weighted imaging. J Magn Reson Imaging 2013; 37: 1260-76.
5. Baliyan V, Das CJ, Sharma R, Gupta AK. Diffusion weighted imaging: Technique and applications. World J Radiol 2016; 8: 785-98.
6. Manetta R, Palumbo P, Gianneramo C, Bruno F, Arrigoni F, Natella R, et al. Correlation between ADC values and Gleason score in evaluation of prostate cancer: multicentre experience and review of the literature. Gland Surg 2019; 8(Suppl 3):216-22.
7. Bozkurt Bostan T, Koç G, Sezgin G, Altay C, Fazıl Gelal M, Oyar O. Value of Apparent Diffusion Coefficient Values in Differentiating Malignant and Benign Breast Lesions. Balkan Med J 2016; 33: 294-300.
8. DeLano MC, Cooper TG, Siebert JE, Potchen MJ, Kuppusamy K. High-b-value diffusion-weighted MR imaging of adult brain: image contrast and apparent diffusion coefficient map features. AJNR Am J Neuroradiol 2000; 21: 1830-6.
9. Bilgili Y, Unal B. Effect of region of interest on interobserver variance in apparent diffusion coefficient measures. AJNR Am J Neuroradiol 2004; 25: 108-11.
10. Thoeny HC, De Keyzer F, Oyen RH, Peeters RR. Diffusion-weighted MR imaging of kidneys in healthy volunteers and patients with parenchymal diseases: initial experience. Radiology 2005; 235: 911-7.
11. Mulkern RV, Barnes AS, Haker SJ, Hung YP, Rybicki FJ, Maier SE, et al. Biexponential Characterization of Prostate Tissue Water Diffusion Decay Curves Over an Extended b-factor Range. Magn Reson Imaging 2006; 24: 563-8.
12. Le Bihan D, Delannoy J, Levin RL. Temperature mapping with MR imaging of molecular diffusion: application to hyperthermia. Radiology 1989; 171: 853-7.
13. Yang X, Lin Y, Xing Z, She D, Su Y, Cao D. Predicting 1p/19q codeletion status using diffusion-, susceptibility-, perfusion-weighted, and conventional MRI in IDH-mutant lower-grade gliomas. Acta Radiol 2020: 62: 1657-65.

14. Yılmaz E, Sarı O, Yılmaz A, Ucar N, Aslan A, Inan I. et al. Diffusion-Weighted Imaging for the Discrimination of Benign and Malignant Breast Masses; Utility of ADC and Relative ADC. J Belg Soc Radiol 2018; 102: 24.
15. Han BH, Park SB, Seo JT, Chun YK. Usefulness of Testicular Volume, Apparent Diffusion Coefficient, and Normalized Apparent Diffusion Coefficient in the MRI Evaluation of Infertile Men With Azoospermia. AJR Am J Roentgenol 2018; 210: 543-8.
16. Gelebek Yılmaz F, Yıldırım AE. Relative Contribution of Apparent Diffusion Coefficient (ADC) Values and ADC Ratios of Focal Hepatic Lesions in the Characterization of Benign and Malignant Lesions. Eur J Ther 2018; 24: 150-7.
17. Barral M, Sebbag-Sfez D, Hoeffel C, Chaput U, Dohan A, Eveno C, et al. Characterization of focal pancreatic lesions using normalized apparent diffusion coefficient at 1.5-Tesla: preliminary experience. Diagn Interv Imaging 2013; 94: 619-27.
18. Do RK, Chandarana H, Felker E, Hajdu CH, Babb JS, Kim D, et al. Diagnosis of liver fibrosis and cirrhosis with diffusion-weighted imaging: value of normalized apparent diffusion coefficient using the spleen as reference organ. AJR Am J Roentgenol 2010; 195: 671-6.
19. Papanikolaou N, Gourtsoyianni S, Yarmenitis S, Maris T, Gourtsoyiannis N. Comparison between two-point and four-point methods for quantification of apparent diffusion coefficient of normal liver parenchyma and focal lesions. Value of normalization with spleen. Eur J Radiol 2010; 73: 305-9.
20. Hong Y, Shi Y, Liao W, Klahr NJ, Xia F, Xu C, et al. Relative ADC measurement for liver fibrosis diagnosis in chronic hepatitis B using spleen/renal cortex as the reference organs at 3 T. Clin Radiol 2014; 69: 581-8.
21. Park SO, Kim JK, Kim KA, Park BW, Kim N, Cho G, et al. Relative apparent diffusion coefficient: determination of reference site and validation of benefit for detecting metastatic lymph nodes in uterine cervical cancer. J Magn Reson Imaging 2009; 29: 383-90.
22. Pakala T, Molina M, Wu GY. Hepatic Echinococcal Cysts: A Review. J Clin Transl Hepatol 2016; 4: 39-46.
23. Devran Aybar M, Karagoz Y, Turna O, Tuzcu G, Buker A. The Contribution of Diffusion Weighted MRI (DWI) and Measured ADC Values in Differentiating Benign and Malignant Liver Masses. Istanbul Med J 2013; 14: 16-9.
24. Caro-Domínguez P, Gupta AA, Chavhan GB. Can diffusion-weighted imaging distinguish between benign and malignant pediatric liver tumors? Pediatr Radiol 2018; 48: 85-93.
25. Parikh T, Drew SJ, Lee VS, Wong S, Hecht EM, Babb JS, et al. Focal liver lesion detection and characterization with diffusion-weighted MR imaging: comparison with standard breath-hold T2-weighted imaging. Radiology 2008; 246: 812-22.
26. Bruegel M, Holzapfel K, Gaa J, Woertler K, Waldt S, Kiefer B, et al. Characterization of focal liver lesions by ADC measurements using a respiratory triggered diffusion-weighted single-shot echo-planar MR imaging technique. Eur Radiol 2008; 18: 477-85.
27. Miller FH, Hammond N, Siddiqi AJ, Shroff S, Khatri G, Wang Y, et al. Utility of diffusion-weighted MRI in distinguishing benign and malignant hepatic lesions. J Magn Reson Imaging 2010; 32: 138-47.
28. Wu XF, Bai XM, Yang W, Sun Y, Wang H, Wu W, et al. Differentiation of atypical hepatic hemangioma from liver metastases: Diagnostic performance of a novel type of color contrast enhanced ultrasound. World J Gastroenterol 2020; 26: 960-72.
29. Nam SJ, Park KY, Yu JS, Chung JJ, Kim JH, Kim KW. Hepatic cavernous hemangiomas: relationship between speed of intratumoral enhancement during dynamic MRI and apparent diffusion coefficient on diffusion-weighted imaging. Korean J Radiol 2012; 13: 728-35.
30. Cui Y, Zhang XP, Sun YS, Tang L, Shen L. Apparent diffusion coefficient: potential imaging biomarker for prediction and early detection of response to chemotherapy in hepatic metastases. Radiology 2008; 248: 894-900.
31. Vaupel P, Mayer A. Hypoxia in cancer: significance and impact on clinical outcome. Cancer Metastasis Rev 2007; 26: 225-39.
32. Rockwell S, Dobrucki IT, Kim EY, Marrison ST, Vu VT. Hypoxia and radiation therapy: past history, ongoing research, and future promise. Curr Mol Med 2009; 9: 442-58.
33. Serša I, Bajd F, Savarin M, Jesenko T, Čemažar M, Serša G. Multiparametric High-Resolution MRI as a Tool for Mapping of Hypoxic Level in Tumors. Technol Cancer Res Treat 2018; 17: 1533033818797066.